Applied Surface Science 280 (2013) 207–211

Contents lists available at SciVerse ScienceDirect

Applied Surface Science

journal homepage: www.elsevier.com/locate/apsusc

Initial reaction of silicon precursors with a varying number of dimethylamino ligands on a hydroxyl-terminated silicon (0 0 1) surface

Yong-Chan Jeong, Seung-Bin Baek, Dae-Hee Kim, Ji-Su Kim, Yeong-Cheol Kim *

School of Energy, Materials & Chemical Engineering, Korea University of Technology and Education, Cheonan 330-708, Republic of Korea

ARTICLE INFO

Article history:
Received 14 January 2013
Received in revised form 24 April 2013
Accepted 24 April 2013
Available online 2 May 2013

Keywords:
Adsorption
Surface reaction
Dimethylamino ligand
Density functional theory
Atomic layer deposition

ABSTRACT

The initial reaction of silicon precursors with a varying number of dimethylamino (—$N(CH_3)_2$) ligands on a hydroxyl-terminated silicon (0 0 1) surface was investigated using density functional theory. Five silicon precursors were chosen to evaluate their adsorption energy and reaction energy barrier as a function of the number of the —$N(CH_3)_2$ ligands: silane (SiH_4), dimethylaminosilane ($SiH_3[N(CH_3)_2]$), *bis*-dimethylaminosilane ($SiH_2[N(CH_3)_2]_2$), *tris*-dimethylaminosilane ($SiH[N(CH_3)_2]_3$), and *tetrakis*-dimethylaminosilane ($Si[N(CH_3)_2]_4$). The adsorption energy increased with the number of the —$N(CH_3)_2$ ligands, while the reaction energy barrier showed a parabolic behavior. We found that $SiH_3[N(CH_3)_2]$, $SiH_2[N(CH_3)_2]_2$, and $SiH[N(CH_3)_2]_3$ could be recommended as the suitable Si precursors due to their high adsorption energies and low reaction energy barriers.

1. Introduction

The deposition technique that can adjust the thickness of thin-films in semiconductor devices on an atomic scale has become essential as the semiconductor devices have shrunk down below 20 nm. Atomic layer deposition (ALD) that is based on sequential and self-limiting surface reaction is the most suitable deposition technique to meet the requirement of the atomic-scale film-thickness accuracy [1]. During the initial ALD stage, the precursors are adsorbed on the surface, react with it via bond breakings and makings, and form reaction products. In order to become a suitable ALD precursor, the adsorption energy of the precursor on the surface should be higher than the reaction energy barrier between the precursor and the surface; otherwise, the precursor would desorb rather than react with the surface [2].

Silicon dioxide (SiO_2) has been fabricated by ALD in order to obtain a high-quality SiO_2 film. Among many silicon (Si) precursors, those that consist of dimethylamino (DMA, —$N(CH_3)_2$) ligands were attractive because the number of DMA ligands affected the reaction between the Si precursors and the surface [3,4]. Kamiyama et al. evaluated *bis*-dimethylaminosilane (BDMAS, $SiH_2[N(CH_3)_2]_2$) and *tris*-dimethylaminosilane (TDMAS, $SiH[N(CH_3)_2]_3$) for SiO_2 ALD and mentioned that BDMAS showed a higher growth rate and lower impurity than TDMAS due to the higher thermal decomposition rate [3]. Similarly, Burton et al. evaluated TDMAS and *tetrakis*-dimethylaminosilane (TeDMAS, $Si[N(CH_3)_2]_4$) for SiO_2 ALD and mentioned that TDMAS showed a better surface reaction than TeDMAS [4]. The reason, they claimed, was that the hydrogen (H) atom bonded to the Si atom in TDMAS relatively reduced the steric hindrance for the surface reaction compared to TeDMAS that contains the four DMA ligands bonded to the Si atom in the precursor.

The adsorption energies and the reaction energy barriers of precursors were calculated using density functional theory (DFT) in order to investigate the reaction of precursors on surfaces. Li et al. reported that TDMAS reacted on a SiO_2 (0 0 1) surface to produce two dimethylamines ($NH(CH_3)_2$s), but they did not consider the adsorption energy of TDMAS on the surface [5]. Baek et al. reported that the nitrogen (N) atom of *bis*-diethylaminosilane ($SiH_2[N(C_2H_6)_2]_2$) reacted with the H atom of a hydroxyl (—OH) on a Si (0 0 1) surface due to a reaction energy barrier that was lower than its adsorption energy [2]. However, the effect of the number of ligands in Si precursors on surface reaction has not been studied systematically yet. In this study, we investigated the initial reaction of Si precursors as a function of the number of DMA ligands on an —OH-terminated Si (0 0 1) surface using DFT with consideration of the van der Waals interaction and the effect of temperature.

2. Calculation details

All calculations were performed using the Vienna *Ab-initio* Simulation Package (VASP) code [6–9] based on DFT. The projector

* Corresponding author at: 1600 Chungjeollo Dongnamgu, Cheonan, Chungnam 330-708, Republic of Korea. Tel.: +82 41 560 1326; fax: +82 41 560 1360.
E-mail addresses: yc21kim@gmail.com, yckim@kut.ac.kr (Y.-C. Kim).

0169-4332/$ – see front matter © 2013 Elsevier B.V. All rights reserved.
http://dx.doi.org/10.1016/j.apsusc.2013.04.129

augmented wave (PAW) method of Blöchl [10] implemented in VASP by Kresse and Joubert [11] was used to describe the ion cores. The exchange correlation energy was described by the generalized-gradient approximation (GGA) of Perdew, Burke, and Ernzerhof (PBE) [12]. All calculations considered the van der Waals interaction based on Grimme's DFT-D2 approach [13]. The effect of temperature on the adsorption energy was considered by using the Joint Army–Navy–Air Force (JANAF) Thermochemical Tables [14]. Since geometric configuration was not well optimized with DFT-D2, all geometric configurations were first optimized using DFT. The cut-off energy of 500 eV and $2 \times 2 \times 1$ k-points mesh with zero shift for a slab structure including a 2-nm thick vacuum layer were used to generate the plane wave basis set with the Monkhorst–Pack grid method [15]. Partial wave occupancies were calculated with the Gaussian smearing method, and its factor was 0.05 eV. Electronic and geometry optimizations were converged when the total energy difference between successive calculation steps was less than 10^{-3} and 10^{-2} eV, respectively. All atoms were allowed to relax until the force on each ion was below 0.02 eV/Å.

The calculated lattice parameter of a Si unit cell was 5.41 Å and was in good agreement with the experimentally measured (5.43 Å) [16] and theoretically calculated (5.41 Å) [17] ones within a 0.4% error. A 4×4 Si (0 0 1) surface with four Si layers was constructed using the optimized Si unit cell. —OHs were attached to the top-layer Si atoms in order to form the —OH-terminated Si (0 0 1) surface that was prepared experimentally to reduce the initial incubation period of the ALD growth [18], and H atoms were attached to the bottom-layer Si atoms in order to remove their dangling bonds. The bottom-layer Si atoms with H atoms underneath were fixed, and the three top Si layers with —OHs on top were allowed to relax. Silane (SiH_4), dimethylaminosilane (DMAS, $SiH_3[N(CH_3)_2]$), BDMAS, TDMAS, and TeDMAS were optimized. The bond dissociation energy in each optimized Si precursor was calculated by breaking the bond while maintaining the rest structure fixed to find a weak bond in the precursor. The Bader analysis method was performed to calculate the electronic charge density of atoms [19,20]. The optimized Si precursors were adsorbed on the surface with consideration of the weak bond breakage during the following chemical reaction, and their reaction energy barrier calculation was performed using the climbing nudged elastic band (CI-NEB) tool implemented in the VASP code [21]. Six images including the initial and final configurations were used for the CI-NEB calculations. Atoms in the relaxed layers and the Si precursors were allowed to relax during the energy barrier calculations.

3. Results and discussion

Fig. 1(a) shows a fully —OH-terminated 4×4 Si (0 0 1) surface with four Si layers. The $Si_{surface}$ and $X_{–OH}$ atom (X = oxygen (O), H) indicate the Si atom and X atom of —OH on the surface, respectively. The bond dissociation energies, bond lengths, and Bader charges of the surface are shown in Table 1. The Si^d atom is the Si atom of the dimer in the surface. The calculated bond lengths were in good agreement with the published data [22]. On the surface, the Bader charges of the Si^d and H atom were positive, while that of the O atom was negative. Fig. 1(b) shows the five optimized Si precursors: silane, DMAS, BDMAS, TDMAS, and TeDMAS. The $X'_{precursor}$ atom (X' = Si, N, carbon (C), and H) indicates the X' atom in the Si precursors. Silane is composed of one Si atom bonded by four H atoms. DMAS, BDMAS, TDMAS, and TeDMAS are formed by replacing one, two, three, and four H atom(s) by the same number of DMA ligand(s), respectively. The DMA ligand consists of one N atom and two methyls (CH_2s). Table 2 shows the average bond dissociation energies, bond lengths, and Bader charges of the five Si precursors. The H^{Si} and H^C atoms are the H atoms bonded to the Si and C atoms,

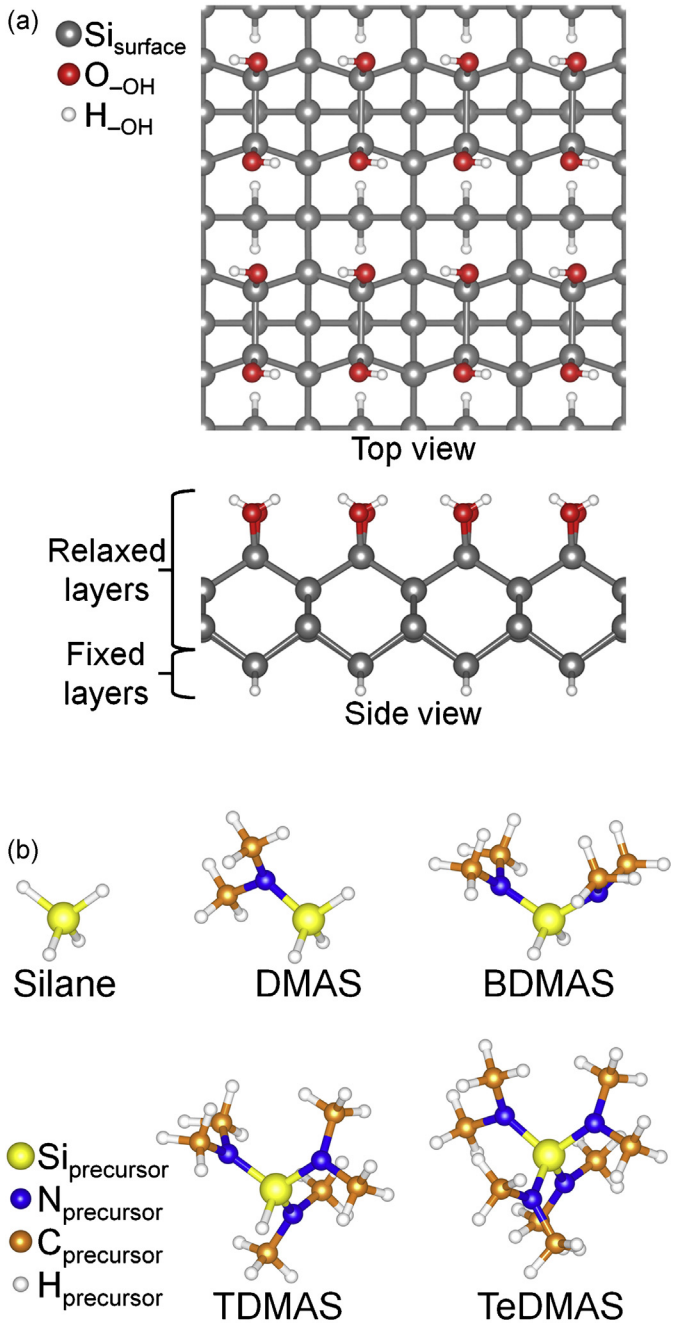

Fig. 1. (a) Top and side views of a fully —OH-terminated Si (0 0 1) surface, and (b) perspective views of the optimized silane, DMAS, BDMAS, TDMAS, and TeDMAS. The $Si_{surface}$ and $X_{–OH}$ (X = O, H) atoms indicate the Si atom and X atom of —OH on the surface, respectively. The $X'_{precursor}$ (X' = Si, N, C, and H) atom indicates the X' atom in the Si precursor.

respectively. Silane had only Si—H bonds with an average Si—H bond dissociation energy of 5.42 eV. DMAS, BDMAS, TDMAS, and TeDMAS precursors showed that the Si—N bond was the weakest among the bonds in each Si precursor with average Si—N bond dissociation energies of 4.87, 4.70, 4.85, and 5.00 eV, respectively. Therefore, the Si—N bond would be easily broken when DMAS, BDMAS, TDMAS, and TeDMAS precursors react with —OH on the surface. In the Si precursors, the Bader charges of the Si, C, and H^C atoms were positive, while those of the N and H^{Si} atoms were negative. As a result, when the Si precursor was adsorbed on the surface, the positive $Si_{precursor}$ atom and negative $H_{precursor}$ atom or the positive $Si_{precursor}$ atom

Table 1
Bond dissociation energies, bond lengths, and Bader charges in the —OH-terminated Si (0 0 1) surface.

Bond dissociation energy (eV)|bond length (Å)			Bader charge		
Si^d—Si^d [a]	Si^d—O	O—H	Si^d	O	H
–|2.43 (2.36)[b]	5.24|1.68 (1.68)	5.56|0.97 (0.97)	3.21	−1.46	0.30

[a] The Si^d atom is the Si atom of the dimer in the surface.
[b] Ref. [22].

Table 2
Bond dissociation energies, bond lengths, and Bader charges in silane, DMAS, BDMAS, TDMAS, and TeDMAS.

Precursor	Bond dissociation energy (eV)|bond length (Å)				Bader charge				
	Si—H^{Si} [a]	Si—N	N—C	C—H^C [a]	Si	N	C	H^{Si}	H^C
Silane	5.43|1.49	–	–	–	2.43	–	–	−0.61	–
DMAS	5.11|1.49	4.87|1.73	5.42|1.46	5.90|1.10	2.59	−1.44	0.25	−0.62	0.03
BDMAS	5.43|1.49	4.70|1.74	5.40|1.46	5.84|1.10	2.74	−1.44	0.29	−0.63	0.02
TDMAS	5.23|1.49	4.85|1.73	5.33|1.45	5.80|1.10	2.85	−1.48	0.28	−0.61	0.03
TeDMAS	–	5.00|1.73	5.39|1.45	5.79|1.10	3.00	−1.46	0.30	–	0.02

[a] The H^{Si} and H^C atoms are the H atoms bonded to the Si and C atoms, respectively.

and negative $N_{precursor}$ atom were attracted to the negative $O_{–OH}$ atom and positive $H_{–OH}$ atom, respectively.

Fig. 2 shows adsorption configurations of the five Si precursors on the surface and their adsorption energies (E_{ad}). The relative energy is set to 0 eV as reference, when the Si precursors are located at a distance of 10 Å from the surface. The five Si precursors were adsorbed on the surface with no energy barrier. Various configurations for silane adsorption on the surface were tried, and the adsorption configuration shown in Fig. 2 resulted in the highest adsorption energy of 0.16 eV when the Si_{silane} and H_{silane} atoms were located on the $O_{–OH}$ and $H_{–OH}$ atoms at $Si_{silane}\cdots O_{–OH}$ and $H_{silane}\cdots H_{–OH}$ distances of 2.89 and 2.33 Å, respectively. Various configurations for DMAS, BDMAS, TDMAS, and TeDMAS adsorption on the surface were also tried, and their optimized adsorption configurations are shown in Fig. 2. The optimized DMAS adsorption configuration resulted in an adsorption energy of 0.59 eV when the Si_{DMAS} and N_{DMAS} atoms were located on the $O_{–OH}$ and $H_{–OH}$ atoms at $Si_{DMAS}\cdots O_{–OH}$ and $N_{DMAS}\cdots H_{–OH}$ distances of 3.03 and 1.74 Å, respectively. The DMAS adsorption energy was higher than that of silane due to the negative Bader charge of the N atom being stronger than that of the H atom. Since BDMAS has two DMA ligands, two optimized adsorption configurations were plausible. The first adsorption configuration ($BDMAS^{1Si\&1N}$) followed the trend of the DMAS adsorption; one N atom of the DMA ligand is attracted to the $H_{–OH}$ atom. At this BDMAS adsorption configuration, the $Si_{BDMAS}\cdots O_{–OH}$ and $N_{BDMAS}\cdots H_{–OH}$ distances were 3.12 and 1.69 Å, respectively, with an adsorption energy of 0.66 eV. Additionally, due to the two N_{BDMAS} atoms, the other optimized BDMAS adsorption configuration ($BDMAS^{2N}$) was obtained when the two N_{BDMAS} atoms were located on the two $H_{–OH}$ atoms at $N_{BDMAS}\cdots H_{–OH}$ distances of 1.83 and 1.84 Å. Though higher adsorption energy was expected due to the two $N_{BDMAS}\cdots H_{–OH}$ attractions, the $BDMAS^{2N}$ adsorption energy was 0.69 eV, which was similar to that of $BDMAS^{1Si\&1N}$. This can be explained by the $N_{BDMAS}\cdots H_{–OH}$ distance of $BDMAS^{2N}$ that is longer than that of $BDMAS^{1Si\&1N}$. The optimized TDMAS and TeDMAS adsorption configurations also followed the trend of the DMAS adsorption. At its TDMAS (TeDMAS) adsorption configuration, the $Si_{TDMAS\ (TeDMAS)}\cdots O_{–OH}$ and $N_{TDMAS\ (TeDMAS)}\cdots H_{–OH}$ distances were 3.20 (3.44) and 1.77 (1.75) Å, respectively, with an adsorption energy of 0.74 (0.84) eV; the numbers in parentheses refer to values for the TeDMAS adsorption. However, when TDMAS and TeDMAS were adsorbed with two DMA ligands close to the surface, its adsorption energy decreased by more than 0.28 eV in comparison with that of the optimized adsorption configurations due to the steric hindrance between the bulky DMA ligands and the surface. Table 3 shows the variation of the bond dissociation energies and the bond lengths at the adsorption configurations. When silane was adsorbed on the surface, the bond dissociation energies decreased a little with no change of the bond lengths. DMAS, BDMAS, TDMAS, and TeDMAS precursors showed a decrease in bond dissociation energies and an increase in bond lengths. Unlike the Si precursors containing the DMA ligand(s), silane exhibited a slight decrease of the bond dissociation energies and no change of the bond lengths. This can be explained by the lower attraction between the H_{silane} and $H_{–OH}$ atoms than that between the $N_{precursor}$ and $H_{–OH}$ atoms.

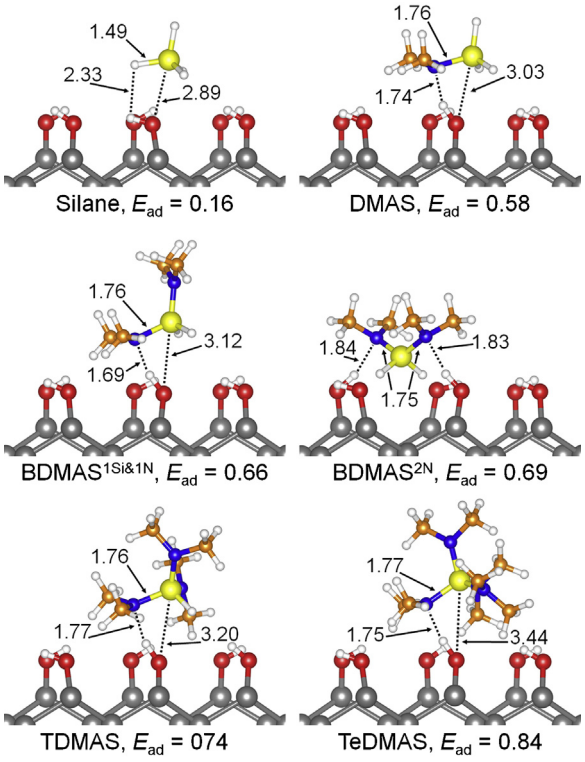

Fig. 2. Adsorption configurations and energies (E_{ad}, eV) of silane, DMAS, BDMAS, TDMAS, and TeDMAS on the surface. BDMAS has two favorable adsorption configurations: $BDMAS^{1Si\&1N}$ and $BDMAS^{2N}$. In the $BDMAS^{1Si\&1N}$ configuration, the Si_{BDMAS} and N_{BDMAS} atoms were located on the $O_{–OH}$ and $H_{–OH}$ atoms, respectively. In the $BDMAS^{2N}$ configuration, the two N_{BDMAS} atoms were located on the two $H_{–OH}$ atoms. The unit values are shown in Å.

Table 3
Bond dissociation energies and bond lengths of the Si precursors and surface before and after the adsorption of the Si precursors on the surface.

Precursor	Adsorption with consideration of	Bond dissociation energy (eV)|bond length (Å) before adsorption		Bond dissociation energy (eV)|bond length (Å) after adsorption	
		Si—*M* (*M* = H, N) in precursor	O—H in surface	Si—*M* (*M* = H, N) in precursor	O—H in surface
Silane	Si—H	5.43|1.49	5.56|0.97	5.38|1.49	5.54|0.97
DMAS	Si—N	4.87|1.73	5.56|0.97	4.70|1.76	5.40|1.01
$BDMAS^{1Si\&1N}$	Si—N	4.70|1.74	5.56|0.97	4.43|1.76	5.34|1.02
$BDMAS^{2N}$	Si—N	4.70|1.74	5.56|0.97	4.52|1.75	5.33|1.00
TDMAS	Si—N	4.85|1.73	5.56|0.97	4.62|1.76	5.36|1.01
TeDMAS	Si—N	5.00|1.73	5.56|0.97	4.69|1.77	5.30|1.02

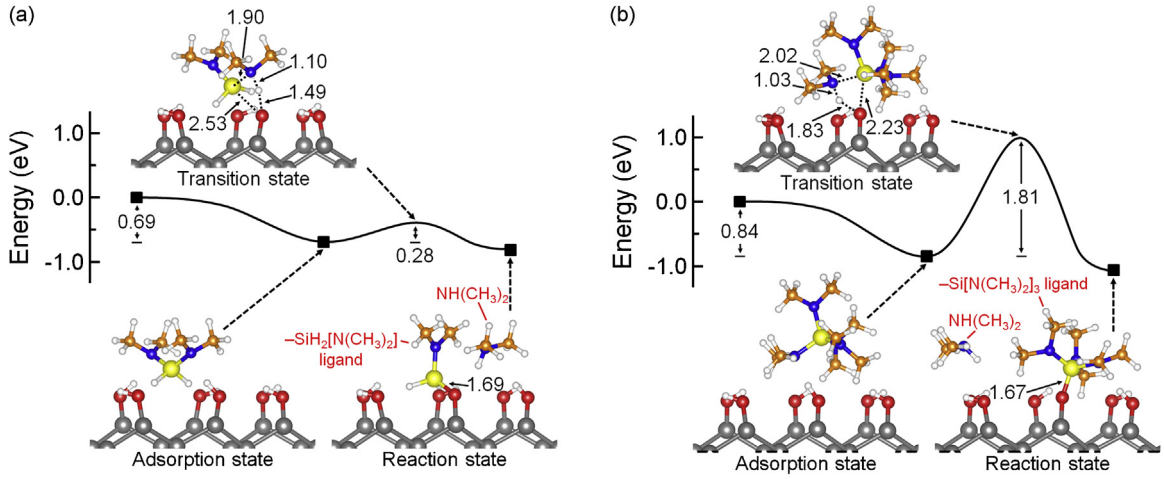

Fig. 3. Energy variations for the (a) BDMAS and (b) TeDMAS reaction with —OH on the surface. The unit values are shown in Å.

Fig. 3(a) shows the $BDMAS^{2N}$ reaction and its energy barrier on the surface. The adsorbed $BDMAS^{2N}$ reacts with —OH on the surface to produce a dimethylaminosilyl ($—SiH_2[N(CH_3)_2]$) ligand and $NH(CH_3)_2$; its chemical reaction equation is shown below:

$$—OH + SiH_2[N(CH_3)_2]_2 \rightarrow —O—SiH_2[N(CH_3)_2] + NH(CH_3)_2.$$

The Si_{BDMAS} atom is bonded to the $O_{–OH}$ atom with a bond length of 1.69 Å. $NH(CH_3)_2$, generated as a by-product, moves away from the $—SiH_2[N(CH_3)_2]$ ligand by a distance of 3.71 Å. The reaction required an energy barrier of 0.28 eV that was lower than the adsorption energy. Fig. 3(b) shows the TeDMAS reaction and its energy barrier on the surface. The adsorbed TeDMAS reacts with —OH on the surface to produce a *tris*-dimethylaminosilyl ($—Si[N(CH_3)_2]_3$) ligand and $NH(CH_3)_2$; its chemical reaction equation is shown below:

$$—OH + Si[N(CH_3)_2]_4 \rightarrow —O—Si[N(CH_3)_2]_3 + NH(CH_3)_2.$$

The Si_{TeDMAS} atom is bonded to the $O_{–OH}$ atom with a bond length of 1.67 Å. $NH(CH_3)_2$, generated as a by-product, moves away from the $—Si[N(CH_3)_2]_3$ ligand by a distance of 5.97 Å. The reaction required an energy barrier of 1.81 eV that was higher than the adsorption energy.

Fig. 4 shows the adsorption energy and reaction energy barrier as a function of the number of DMA ligands. From the adsorption energies shown in Fig. 2, the adsorption energy increased significantly when one H atom was replaced by one DMA ligand, while replacement of more than one DMA ligand showed less increase in adsorption energy. However, the adsorption energies shown in Fig. 2 were obtained at 0 K. Typically, the surface reaction of a precursor should consider the effect of temperature due to the entropy change via the adsorption of the precursor; when the precursor was adsorbed on the surface, the adsorbed precursor would lose degrees of freedom. In order to consider the effect of temperature on the surface reaction of a precursor, the entropy of the gas-phase precursor was estimated by using the JANAF Thermochemical Tables [14]; the entropy energy (*TS*) of the gas-phase silane at a typical ALD condition (*P* = 1 Torr, *T* = 600 K) was calculated to be 1.85 eV. The curve of the adsorption energy with consideration of the entropy energy would shift downwardly as shown by the red-lined curve in Fig. 4, if we assume that all other Si precursors show the same entropy energy of silane. (For interpretation of the references to

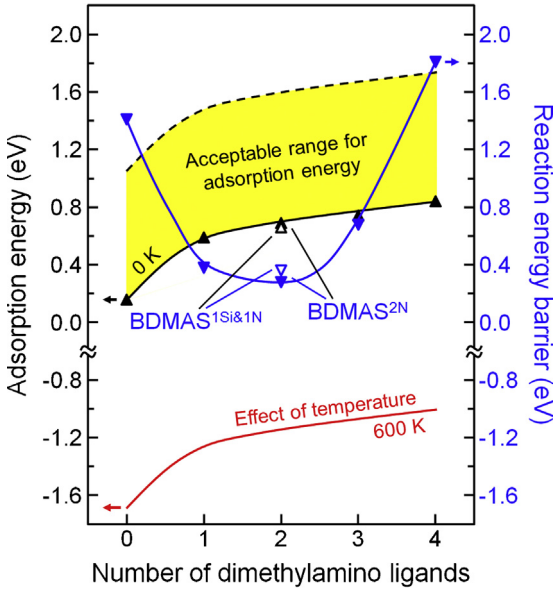

Fig. 4. Adsorption energy and reaction energy barrier as a function of the number of DMA ligands. The effect of temperature is considered for the adsorption energy.

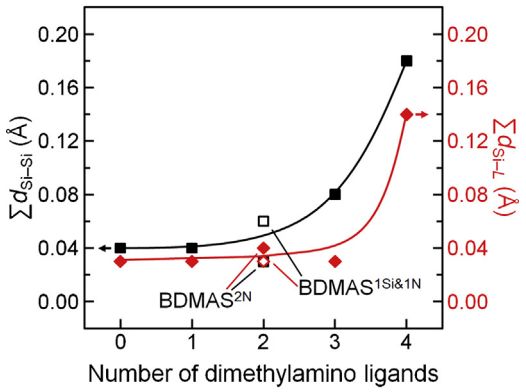

Fig. 5. Variation of bond lengths as a function of the number of DMA ligands. $\sum d_{Si-Si}$ indicates the sum of the variation of the Si—Si bond lengths near the reaction site on the surface and $\sum d_{Si-L}$ indicates the sum of the variation of the Si—ligand bond lengths in the Si precursors.

color in text, the reader is referred to the web version of this article.) The reaction energy barrier showed a parabolic behavior; more details will be explained in Fig. 5. Based on the adsorption energies with the consideration of the effect of temperature, all Si precursors would not react on the surface because the reaction energy barrier is higher than the adsorption energy. We know that BDMAS and TDMAS are experimentally suitable Si precursors while silane and TeDMAS are not for SiO_2 ALD [3,4]. From these experimental results, an acceptable range for the curve of the adsorption energy is found, as shown in Fig. 4, to be in agreement with the experimental results. Based on the acceptable range for the curve of the adsorption energy, the adsorption energy of DMAS would be higher than the reaction energy barrier; this indicates that DMAS would be a good Si precursor for SiO_2 ALD.

The reaction energy barrier decreased from 1.42 to 0.28 eV when the number of DMA ligands increased from zero to two (Fig. 4). This behavior was acceptable due to the increase of the adsorption energy with the number of DMA ligands and the decrease of the bond dissociation energy. However, when the number of DMA ligands became more than two, the reaction energy barrier started to increase. In order to consider the effect of strain energy on the reaction energy barrier, the variation of the bond lengths on the surface and the Si precursors at the transition configuration was calculated, as shown in Fig. 5. $\sum d_{Si-Si}$ indicates the sum of the variation of the Si—Si bond lengths near to the reaction site on the surface, and $\sum d_{Si-L}$ indicates the sum of the variation of the Si—ligand bond lengths in the Si precursors. $\sum d_{Si-Si}$ did not change when the number of DMA ligands increased from zero to one; the Si precursor is changed from silane to DMAS. Replacement of two DMA ligands for BDMAS showed two different values of $\sum d_{Si-Si}$. The $\sum d_{Si-Si}$ of BDMAS$^{1Si\&1N}$ was higher, while that of BDMAS^{2N} was lower than that of DMAS. $\sum d_{Si-Si}$ increased when the number of DMA ligands became more than two. $\sum d_{Si-L}$ did not change when the number of DMA ligands increased from zero to three. However, when the number of DMA ligands increased from three to four, $\sum d_{Si-L}$ increased significantly. Therefore, the increase of the reaction energy barrier with the number of DMA ligands can be attributed to the strain energy increase by the increase of $\sum d_{Si-Si}$ and $\sum d_{Si-L}$.

4. Conclusions

We studied the initial reaction of Si precursors as a function of the number of DMA ligands on the —OH-terminated Si (0 0 1) surface using DFT. The adsorption energy of the Si precursors on the surface increased significantly when the number of DMA ligands increased from zero to one. This is mainly due to one N atom of the DMA ligand. The reaction energy barrier of the Si precursors with the surface showed a parabolic behavior. The decrease of the reaction energy barrier could be explained by the increase of the adsorption energy and the decrease of the bond dissociation energy when the number of DMA ligands is less than two. The increase of the reaction energy barrier with replacement of more than two DMA ligands was explained through the increase of the strain energy estimated by the greater variation of the bond lengths. From these calculations, we would recommend DMAS as a suitable precursor in addition to the experimentally proven BDMAS and TDMAS among the five tested Si precursors.

References

[1] S.M. George, Chemical Reviews 100 (2010) 111–131.
[2] S.-B. Baek, D.-H. Kim, Y.-C. Kim, Applied Surface Science 258 (2012) 6341–6344.
[3] S. Kamiyama, T. Miura, Y. Nara, Thin Solid Films 515 (2006) 1517–1521.
[4] B.B. Burton, S.W. Kang, S.W. Rhee, S.M. George, Journal of Physical Chemistry C 113 (2009) 8249–8257.
[5] J.Y. Li, J.P. Wu, C.G. Zhou, B. Han, E.J. Karwacki, M.C. Xiao, X.J. Lei, H.S. Cheng, Journal of Physical Chemistry C 113 (2009) 9731–9736.
[6] G. Kresse, J. Hafner, Physical Review B 47 (1993) 558–561.
[7] G. Kresse, Technische Universiät Wien, 1993 (Thesis).
[8] G. Kresse, J. Furthmüller, Computation Materials Science 6 (1996) 15–50.
[9] G. Kresse, J. Furthmüller, Physical Review B 54 (1996) 11169–11186.
[10] P.E. Blöchl, Physical Review B 50 (1994) 17953–17979.
[11] G. Kresse, D. Joubert, Physical Review B 59 (1999) 1758–1775.
[12] J.P. Perdew, K. Burke, M. Ernzerhof, Physical Review Letters 77 (1996) 3865–3868.
[13] S.J. Grimme, Journal of Computational Chemistry 27 (2006) 1787–1799.
[14] M.M. Chase Jr., NIST-JANAF Thermochemical Tables, 4th ed., American Institute of Physics, New York, 1998.
[15] H.J. Monkhorst, J.D. Pack, Physical Review B 13 (1976) 5188–5192.
[16] R.O.A. Hall, Acta Crystallographica 14 (1961) 1004–1005.
[17] T. Bučko, J. Hafner, S. Lebégue, J.G. Ángyán, Journal of Physical Chemistry A 114 (2010) 11814–11824.
[18] S.S. Lee, J.Y. Baik, K.-S. An, Y.D. Sub, J.-H. Oh, Y.S. Kim, Journal of Physical Chemistry B 108 (2004) 15128–15132.
[19] G. Henkelman, A. Arnaldsson, H. Jónsson, Computation Materials Science 36 (2006) 354–360.
[20] E. Sanville, S.D. Kenny, R. Smith, G. Henkelman, Journal of Computational Chemistry 28 (2007) 899–908.
[21] D. Sheppard, R. Terrell, G. Henkelman, Journal of Chemical Physics 128 (2008) 134106–134115.
[22] G. Demirel, M. Çakmak, T. Çaykara, Ş. Ellialtıoğlu, Journal of Physical Chemistry C 111 (2007) 15020–15025.